J Mater Sci: Mater Electron (2013) 24:5111–5116
DOI 10.1007/s10854-013-1531-5

Molten salt synthesis and photoluminescence properties of novel red emitting phosphors $Ba_5(VO_4)_3Cl:Eu^{3+},K^+$

Zhanggen Xia · Yujun Liang · Wenzhu Huang · Mengfei Zhang · Dongyan Yu · Jiamin Wu · Jianwen Zhao · Miaohui Tong · Qiang Wang

Received: 19 August 2013 / Accepted: 3 October 2013 / Published online: 11 October 2013

Abstract A series of $Ba_5(VO_4)_3Cl:Eu^{3+},K^+$ phosphors have been synthesized by the molten salt synthesis method. The crystalline structure, morphology, photoluminescence properties and lifetimes were characterized using X-ray diffraction (XRD), field emission scanning electron microscope (FE-SEM) and photoluminescence spectroscopy, respectively. XRD indicates that the $Ba_5(VO_4)_3Cl:Eu^{3+},K^+$ phosphors are synthesized successfully via molten salt method. SEM image demonstrates that the obtained phosphors have hexagonal polyhedron morphology. The photoluminescence spectra reveal that the as-prepared phosphors exhibit a bright red emission under the excitation of blue or near ultraviolet light. The concentration quenching was also investigated, and the dipole–dipole interaction is responsible for the concentration quenching of fluorescence emission of Eu^{3+} ions in $Ba_5(VO_4)_3Cl$ phosphor. The present work suggests that the $Ba_5(VO_4)_3Cl:Eu^{3+},K^+$ phosphors would be a potential candidate for light emitting devices.

1 Introduction

As a hot topic in the area of displays, lanthanide ion and transition-metal ion doped phosphors have attracted great interest due to their extraordinary luminous efficiency and irreplaceable in light-emitting devices, such as cathode ray tubes (CRTs), plasma display panels (PDPs), field emission displays (FEDs), and white-light emitting diodes (w-LEDs) [1–6]. The red luminescence of Eu^{3+} ions has been extensively studied as an activator ion because of its distinct 4f–4f transitions. The f-electrons of Eu^{3+} ions are well shielded from the chemical environment and own almost retained atomic character. In consequence, Eu^{3+} ions have been widely used as the luminescent activator for a considerable number of phosphors such as $Y_2O_3:Eu^{3+}$, $Y_2O_2S:Eu^{3+}$, $YVO_4:Eu^{3+}$, $YBO_3:Eu^{3+}$ belonging to the main red emissive components for trichromatic fluorescence materials.

Vanadate is an important class of materials that have been investigated as the phosphor hosts. In general terms, these properties are observed when the hosts are doped with europium and other rare earth ions. Choi et al. [7] synthesized Eu^{3+} doped $Ca_3Sr_3(VO_4)_4$ phosphors via solid state reaction, the emission intensity excited at 329 nm is 221 % as high as that of $Y_2O_3:Eu^{3+}$ excited at 254 nm. Rao et al. [8] prepared $Ca_3La(VO_4)_3:Eu^{3+}$ by a chemical co-precipitation method, and the red-emitting phosphor exhibits an intense narrow line emission at 618 nm under the excitation of 305 nm. Wang et al. [9] fabricated $YVO_4:Eu^{3+}$ nanocrystallines using molten salt synthesis (MSS) method, and investigated the energy transfer from the charge transfer band of V–O to Eu^{3+} ions.

$Ba_5(VO_4)_3Cl$ crystallizes in the well-known apatite structure type, with space group $P6_3/m$, $a = 10.5468$ Å, $c = 7.7437$ Å and $Z = 2$. The crystal structure contains isolated $(VO_4)^{3-}$ tetrahedrons that are bridged by Ba^{2+} ions. The intermediate Cl^- anions, situated on positions with $\bar{3}$ symmetry, are octahedrally surrounded by Ba^{2+} cations

Z. Xia · Y. Liang
Engineering Research Center of Nano-Geomaterials of Ministry of Education, China University of Geosciences, Wuhan 430074, People's Republic of China

Z. Xia · Y. Liang (✉) · W. Huang · M. Zhang · D. Yu · J. Wu · J. Zhao · M. Tong · Q. Wang
Faculty of Materials Science and Chemistry, China University of Geosciences, Wuhan 430074, People's Republic of China
e-mail: yujunliang@sohu.com

[10]. In the apatite structure there are two types of cationic site (M_1 and M_2), the first type of site M_1 has trigonal symmetry due to the tricapped trigonal prism formed by nine oxygen atoms surrounding the cationic site, and the second type of z inversion symmetric octahedron M_2 is seven coordinated with five oxygen atoms and two X^- ions.

It is well-known that the apatite type $Sr_5(PO_4)_3Cl$ is unsurpassed as a phosphor host-matrix and Eu^{2+} doped $Sr_5(PO_4)_3Cl$ has been used as a commercial blue-emitting phosphor in the past decades [11–13]. However, to the best of our knowledge, there is no report devoting to the preparation of chloro-vanadato-apatites $Ba_5(VO_4)_3Cl$ by the MSS method and the photoluminescence (PL) properties of Eu^{3+} doped $Ba_5(VO_4)_3Cl$ phosphors. In this work, the applicability of a simple MSS method for preparation of $Ba_5(VO_4)_3Cl:Eu^{3+}$ was examined to overcome this gap, and the PL properties were investigated in details.

2 Experimental

The $Ba_5(VO_4)_3Cl:Eu^{3+},K^+$ phosphors were synthesized by the MSS method. $BaCO_3$ (A.R), $BaCl_2{\cdot}2H_2O$ (A.R), NH_4VO_3 (A.R), KCO_3 (A.R) and Eu_2O_3 (99.99 %) were used as the raw materials. The stoichiometric amounts of starting materials were weighted and mixed in an agate mortar and an appropriate weight of KCl (A.R) was added as the molten salt. After adequately grinding, the powders were transferred to alumina crucibles and calcined at 900 °C for 3 h. The resulting powders were thoroughly washed with distilled water and ethyl alcohol to remove residual potassium salt and dried at 110 °C.

The crystal structure of the phosphors was characterized by X-ray powder diffractometer (XRD) (Bruker D8 Focus) with Cu–kα ($\lambda = 1.540598$ Å) radiation at 40 kV and 40 mA. The morphology and microstructure were characterized with Japan SU8010 field emission scanning electron microscope (FE-SEM) at 5 kV, 10 μA. Excitation and emission spectra were measured by fluorescence spectrometer (FLUOROMAX-4) with a 150 W xenon lamp as excitation source. The lifetime was recorded on a spectrofluorometer (HORIBA, JOBIN YVON FL3-21), and the 355 nm pulse laser radiation (nano-LED) was used as the excitation source. All the measurements were carried out at room temperature.

3 Results and discussion

3.1 Crystal structure and morphology

Figure 1 displays the XRD patterns of the samples $Ba_{5-2x}(VO_4)_3Cl:xEu^{3+},xK^+$ ($x = 0.30$, 0.40, 0.70, 0.90, 1.00 1.10, 1.20, 1.30, 1.40, 1.60) as a function of Eu^{3+} concentrations x, it can be found that the impurity peaks of $EuVO_4$ are detected after the concentration of Eu^{3+} increases to 0.70, which are marked with ◆, as shown in Fig. 1a. Except for the peaks of $EuVO_4$, all the other diffraction peaks of the selected samples are in good agreement with the ICSD 170769 standard card of $Ba_5(VO_4)_3Cl$ and no characteristic peaks from any other impurities are detected. It indicates that the main phase of the obtained samples adopts the same structure as $Ba_5(VO_4)_3Cl$, illuminating that the dopants are dissolved in the $Ba_5(VO_4)_3Cl$ host and do not cause any detectable change in the host structure. However, the positions of the diffraction peaks are observed gradually move to the high degree with the increase of Eu^{3+} contents (x) from 0.30 to 1.60. Figure 1b clearly presents the three strongest diffraction peaks [(211), (112) and (300)]. It is observed that the three peaks vary to the high degree gradually as increasing the Eu^{3+} doping concentration, and the largest distance is about 0.5°, i.e., the lattice parameters of $Ba_5(VO_4)_3Cl:xEu^{3+},xK^+$ decrease monotonously with increasing in Eu^{3+} doping. The reason is probably attributed to the substitution of Ba^{2+} ($R_{Ba} = 1.35$ Å) with large ionic radius by Eu^{3+} ($R_{Eu} = 0.947$ Å) with small ionic radius.

Figure 2 shows the representative SEM image and EDS of $Ba_{2.80}(VO_4)_3Cl:1.10Eu^{3+},1.10K^+$ phosphor prepared at 900 °C for 3 h by MSS method. The SEM image reveals that the particles have good dispersion. There are mainly two morphologies in the image. Most of the particles which are 5–20 μm in size have hexagonal polyhedron morphology, and the smaller ones are spherical-like. EDS confirms that the hexagonal polyhedron particles are $Ba_5(VO_4)_3Cl:Eu^{3+},K^+$ which is consistent with the XRD pattern.

Generally, the MSS mechanism is a two-step process consisting of particle nucleation and particle growth [14]. The nucleation process depends on the difference of dissolution rates between the reacting oxides in the molten salt. The morphologies of particles mainly depend on the particle growth process [15, 16]. Particle growth can be initiated in two ways when solid particles are dispersed in a liquid matrix: by an interfacial reaction controlled mechanism and a diffusion controlled mechanism. The particles grow into spherical shapes under the diffusion controlled mechanism and into faceted shapes under the interfacial reaction controlled mechanism. Therefore, the interfacial reaction controlled mechanism plays an important role in the synthesis of $Ba_5(VO_4)_3Cl$ particles. Additionally, the author implies that the small spherical-like particles are precipitated from the molten salt in the cooling process.

3.2 Photoluminescence properties

The excitation spectrum of $Ba_{2.80}(VO_4)_3Cl:1.10Eu^{3+},1.10K^+$ phosphor synthesized by MMS method is displayed in Fig. 3.

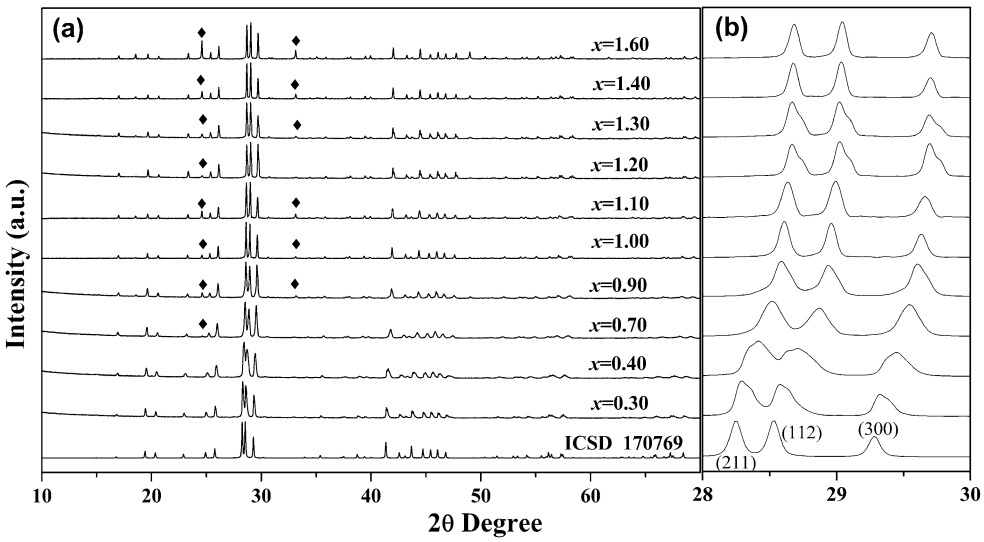

Fig. 1 XRD patterns of the $Ba_{5-2x}(VO_4)_3Cl{:}xEu^{3+},xK^+$ phosphors and ICSD standard card

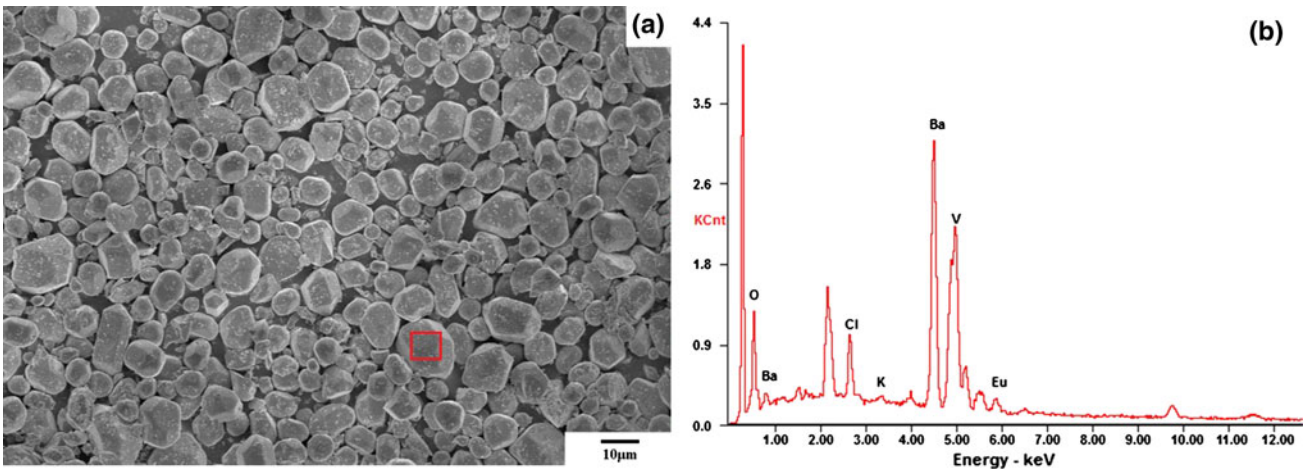

Fig. 2 FE-SEM image (**a**) and EDS (**b**) of $Ba_{2.80}(VO_4)_3Cl{:}1.10Eu^{3+},1.10K^+$ phosphor

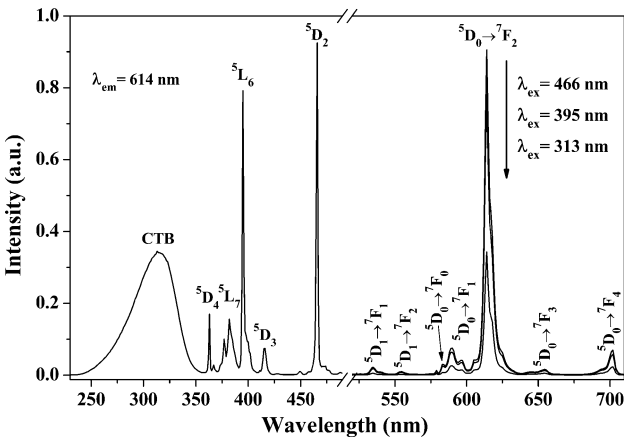

Fig. 3 Photoluminescence spectra of $Ba_{2.80}(VO_4)_3Cl{:}1.10Eu^{3+},1.10K^+$ phosphors

The excitation spectrum monitored at 614 nm consists of a broad excitation band in the vicinity of 220–350 nm and five sharp 4f transition lines of Eu^{3+}, which cover the ranges from long-wavelength UV to visible blue-light region (350–500 nm). The broad band centered at 313 nm is the charge transfer band (CTB) of Eu^{3+}–O^{2-} interaction. In addition to the CTB, five more sharp excitation peaks at 363, 382, 395, 416 and 466 nm are also realized, which are attributed to the direct absorption of the Eu^{3+} ions assigned to transitions of $^7F_0 \rightarrow {}^5D_4$, $^7F_0 \rightarrow {}^5L_7$, $^7F_0 \rightarrow {}^5L_6$, $^7F_0 \rightarrow {}^5D_3$ and $^7F_0 \rightarrow {}^5D_2$, respectively [17, 18]. One of the interesting results of this work is that the phosphors could be strongly excited both by the near-UV light at 395 nm ($^7F_0 \rightarrow {}^5L_6$) and blue light at 466 nm ($^7F_0 \rightarrow {}^5D_2$), thus making the synthesized phosphors suitable for solid-state light sources. Moreover, the peak at 466 nm dominates the excitation spectrum, followed by the peak at 395 nm and the CTB.

The emission spectra achieved by 313, 395 and 466 nm excitation exhibit similarities by comparing the relative intensities of the emission lines from Eu^{3+} 4f–4f transitions corresponding to the transitions from the excited $^5D_0$ level to the ^7F_J ($J = 0$–4) levels of $4f^6$ configuration. The dominated red emission of 614 nm is attributed to the electric dipole transition $^5D_0 \rightarrow {}^7F_2$, indicating that Eu^{3+} is located at the site of non-inversion symmetry [19]. This is in agreement with the crystal structure where the Eu^{3+} ions take of the M sites in the $Ba_5(VO_4)_3Cl$ host lattice without inversion center. Two emission peaks at about 535 and 554 nm corresponding to the $^5D_1 \rightarrow {}^7F_1$ and $^5D_1 \rightarrow {}^7F_2$ transitions are very weak due to the high energy phonons. They can be attributed to the resonant cross-relaxation process such as Eu^{3+} ($^5D_1$) + Eu^{3+} ($^7F_0$) $\rightarrow$ Eu^{3+} ($^5D_0$) + Eu^{3+} ($^7F_3$) [20–22].

In order to investigate the concentration quenching behavior of $Ba_5(VO_4)_3Cl:Eu^{3+},K^+$ phosphors, a series of $Ba_{5-2x}(VO_4)_3Cl:xEu^{3+},xK^+$ phosphors were prepared via MMS method. Figure 4 depicts the emission spectra of $Ba_{5-2x}(VO_4)_3Cl:xEu^{3+},xK^+$ ($x = 0.30$, 0.40, 0.70, 0.90, 1.00, 1.10, 1.20, 1.30, 1.40, 1.60) phosphors. It can be observed that all the emission spectra excited at 466 nm show roughly the same position of emission peaks, except for the intensity. The insert illustrates the dependence of integrated emission intensities for the transitions originating from ^5D_J ($J = 0$–4) levels on Eu^{3+} concentrations. It is seen that the integrated emission intensities increase with the increasing concentration of Eu^{3+} before the maximum intensity, and then reduce at higher concentrations due to concentration quenching; the optimal concentration of Eu^{3+} is 1.10. The concentration quenching behavior in the case of electric multiple interaction between luminescent centers has been quantitatively expressed by Van Uitert's model. In this model, the relationship between the fluorescent intensities and their corresponding doping concentrations of the luminescent center can be mathematically represented as follows [23]:

$$I = \frac{x}{K(1 + \beta x^{Q/3})} \tag{1}$$

where I is the integral emission intensity, x is the luminescent center concentration; K and β are constants for a certain system; Q represents the interaction mechanism between rare earth ions, $Q = 3$, 6, 8 or 10 for exchange, electric dipole–dipole (d–d), electric dipole–quadrupole (d–q) or electric quadrupole–quadrupole (q–q) interactions, respectively. Equation (1) can approximately be reduced to Eq. (2) for $\beta x^{Q/3} \gg 1$:

$$\lg\left(\frac{I}{x}\right) = -\frac{Q}{3}\lg x + A(A = \lg K - \lg \beta) \tag{2}$$

The curve of $\lg(I/x)$ versus $\lg x$ in $Ba_5(VO_4)_3Cl:Eu^{3+},K^+$ phosphor based on Fig. 4 is shown in Fig. 5. Obviously, an approximately linear relation between $\lg I/x$ and $\lg x$ can be found and the slope is about -2.2. The Q value can be calculated as 6.6 based on the linear fitting by using Eq. (1), which is close to 6. Thus, this result indicates that the electric d–d interaction is the major mechanism for the concentration quenching of fluorescence emission of Eu^{3+} ions in $Ba_5(VO_4)_3Cl$ phosphor.

The kinetic decay curve for the representative emission of Eu^{3+} (614 nm, $^5D_0 \rightarrow {}^7F_2$) in $Ba_{4.20}(VO_4)_3Cl:0.40Eu^{3+}$, $0.40K^+$ was measured, as shown in Fig. 6. The decay curve for $^5D_0 \rightarrow {}^7F_2$ (614 nm) of Eu^{3+} can be well fitted with a double exponential function: [24, 25]

$$I = A_1 \exp(-t/\tau_1) + A_2 \exp(-t/\tau_2) \tag{3}$$

where I is the luminescence intensity at time t, t is the time, A_1 and A_2 are constants, and τ_1 and τ_2 are the decay times for the exponential components. Moreover, the average lifetime (τ) can be determined using the calculation below:

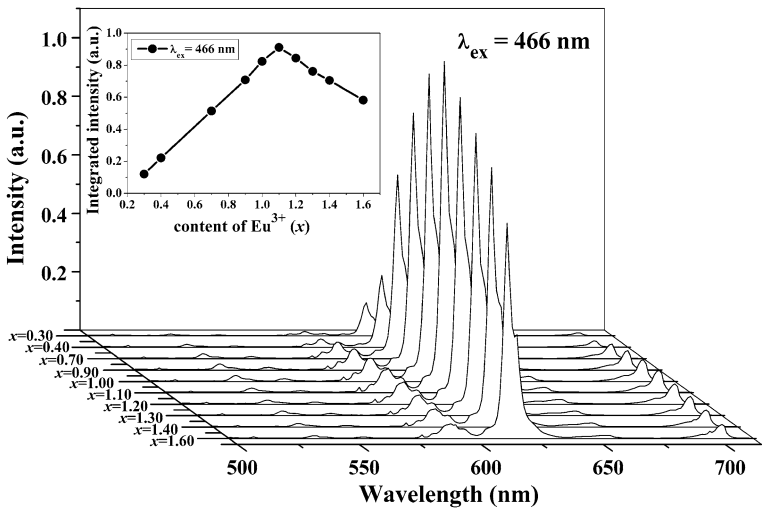

Fig. 4 Emission spectra of $Ba_{5-2x}(VO_4)_3Cl:xEu^{3+},xK^+$ ($x = 0.30$, 0.40, 0.70, 0.90, 1.00, 1.10, 1.20, 1.30, 1.40, 1.60) phosphors on Eu^{3+} doping content (x), the *inset* shows the dependence of integrated emission intensity on the concentration of Eu^{3+} in $Ba_{5-2x}(VO_4)_3Cl:xEu^{3+},xK^+$ with $\lambda_{ex} = 466$ nm

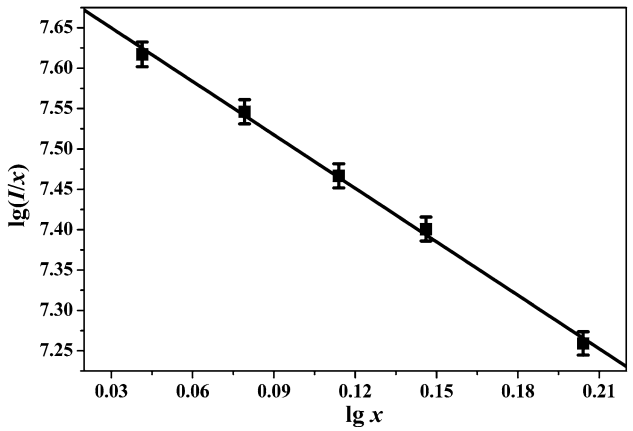

Fig. 5 The curve of lgI/x versus lg$x$ in $Ba_{5-2x}(VO_4)_3Cl{:}xEu^{3+},xK^+$ phosphors ($\lambda_{ex} = 378$ nm)

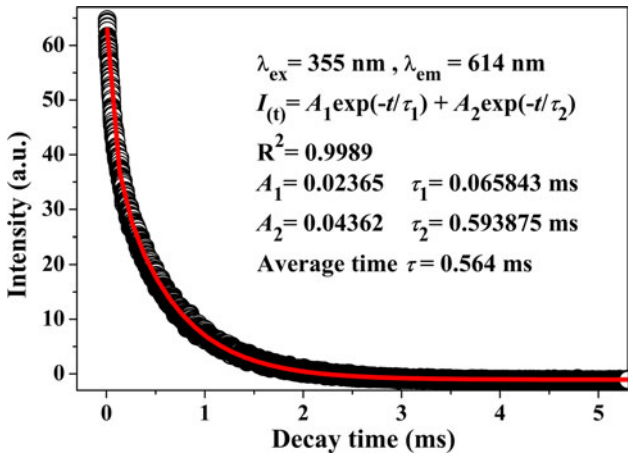

Fig. 6 Decay curves of Eu^{3+} (614 nm, $^5D_0 \rightarrow {}^7F_2$) in $Ba_{4.20}(VO_4)_3Cl{:}0.40Eu^{3+},0.40K^+$

$$\tau = (A_1\tau_1^2 + A_2\tau_2^2)/(A_1\tau_1 + A_2\tau_2) \quad (4)$$

Consequently, it can be seen from Fig. 6 that the average lifetime of Eu^{3+} at 614 nm was determined to be 0.564 ms. In addition, the decay curve indicates that there are two different luminescence centers existing in the $Ba_{4.20}(VO_4)_3Cl{:}0.40Eu^{3+},0.40K^+$ phosphor. And this result implies that Eu^{3+} randomly occupied M_1 and M_2 site in the $Ba_5(VO_4)_3Cl$ host lattice.

Figure 7 represents the CIE 1931 chromaticity coordinates of $Ba_{2.80}(VO_4)_3Cl{:}1.10Eu^{3+},1.10K^+$ phosphor which were calculated based on the corresponding emission spectrum. The CIE coordinates of $Ba_{2.80}(VO_4)_3Cl{:}1.10Eu^{3+},1.10K^+$ phosphor is (0.652, 0.347) which is so close to the NTSC standard value (0.67, 0.33). And no significant change can be observed while varying the concentration of Eu^{3+}.

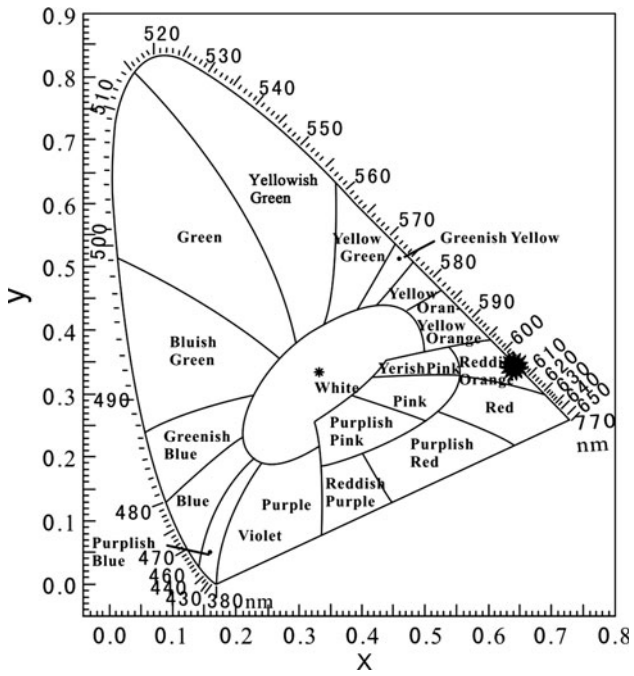

Fig. 7 The CIE 1931 chromaticity coordinates of $Ba_{2.80}(VO_4)_3Cl{:}1.10Eu^{3+},1.10K^+$ phosphor

4 Conclusions

In summary, the novel red emitting phosphors $Ba_{5-2x}(VO_4)_3Cl{:}xEu^{3+},xK^+$ were obtained via the MSS method at 900 °C for 3 h. The as-prepared phosphors have hexagonal polyhedron morphology and exhibit a bright red emission under blue or near-ultraviolet excitation. The present work suggests that the novel phosphors could be a potential candidate for light emitting devices. However, the morphology and particle size distribution are less than satisfactory. In the further work, composite molten salt and the rate of molten salt and raw materials would be employed to improve the morphology and particle size distribution of $Ba_5(VO_4)_3Cl{:}Eu^{3+}$ phosphors.

Acknowledgments This work was supported by the National Natural Science Foundation of China (Grant No. 21171152), the Guangdong Province Enterprise–University–Academy Collaborative Project (No. 2012B091100474) and the Teaching Laboratory Foundation of China University of Geosciences, Wuhan (No. SKJ2012098).

References

1. G.G. Li, X.G. Xu, C. Peng, M.M. Shang, D.L. Geng, Z.Y. Cheng, J. Chen, J. Lin, Opt. Express **19**, 17 (2011)
2. W.J. Park, M.K. Jung, D.H. Yoon, Sens. Actuators B: Chem. **126**, 1 (2007)
3. S. Tonzani, Nature **459**, 7245 (2009)

4. S. Ye, F. Xiao, Y.X. Pan, Y.Y. Ma, Q.Y. Zhang, Mater. Sci. Eng. R **71**, 1 (2010)
5. C.C. Lin, R.S. Liu, J. Phys. Chem. Lett. **2**, 11 (2011)
6. C.C. Lin, Z.R. Xiao, G.Y. Guo, T.S. Chan, R.S. Liu, J. Am. Chem. Soc. **132**, 9 (2010)
7. S. Choi, Y.M. Moon, K. Kim, H.K. Jung, S. Nahm, J. Lumin. **129**, 9 (2009)
8. B.V. Rao, K. Jang, H.S. Lee, S.S. Yi, J.H. Jeong, J. Alloys Compd. **496**, 1–2 (2010)
9. F. Wang, C.L. Liu, Z.Q. Zhou, P.Y. Jia, J. Lin, J. Rare Earths **30**, 3 (2012)
10. Y.H. Roh, S.T. Hong, Acta Crystallogr. Sect. E: Struct. Rep. Online **61**, 8 (2005)
11. Y.X. Zhou, R. Shu, X.Y. Zhang, J.Y. Shi, Z.F. Han, Mater. Sci. Eng. B **68**, 1 (1999)
12. S.J. Dhoble, J. Phys. D Appl. Phys. **33**, 2 (2000)
13. Y.H. Song, H.P. You, M. Yang, Y.H. Zheng, K. Liu, G. Jia, Y.J. Huang, L.H. Zhang, H.J. Zhang, Inorg. Chem. **49**, 4 (2010)
14. H. Jiang, X. Wang, G. Hao, L. Wang, J. Mater. Sci.: Mater. Electron. **24**, 2 (2012)
15. Y.F. Liu, Y.N. Lu, M. Xu, L.F. Zhoun, J. Am. Ceram. Soc. **90**, 6 (2007)
16. H.L. Li, Z.N. Du, G.L. Wang, Y.C. Zhang, Mater. Lett. **64**, 3 (2010)
17. I. Omkaram, B. Vengala Rao, S. Buddhudu, J. Alloys Compd. **474**, 1–2 (2009)
18. A. Katelnikovas, J. Plewa, S. Sakirzanovas, D. Dutczak, D. Enseling, F. Baur, H. Winkler, A. Kareiva, T. Jüstel, J. Mater. Chem. **22**, 41 (2012)
19. F.P. Du, R. Zhu, Y.L. Huang, Y. Tao, H.J. Seo, Dalton Trans. **40**, 43 (2011)
20. G.Z. Li, Z.L. Wang, M. Yu, Z.W. Quan, J. Lin, J. Solid State Chem. **179**, 8 (2006)
21. H.Y. Lin, Y.C. Fang, X.R. Huang, S.Y. Chu, J. Am. Ceram. Soc. **93**, 1 (2010)
22. N.M. Zhang, C.F. Guo, H. Jing, Rsc Adv. **3**, 20 (2013)
23. F. Yang, Y.J. Liang, Y.Z. Lan, W.J. Gao, M.Y. Liu, X.J. Li, W.Z. Huang, Y.L. Li, Z.G. Xia, Mater. Lett. **83** (2012)
24. M.M. Shang, G.G. Li, D.M. Yang, X.J. Kang, C.M. Zhang, J. Lin, J. Electrochem. Soc. **158**, 4 (2011)
25. Z.G. Xia, J.Q. Zhuang, L.B. Liao, Inorg. Chem. **51**, 13 (2012)